



# Design, optimization and comparative analysis of T-shape slot loaded microstrip patch antenna using PSO

Ramesh Kumar Verma<sup>1</sup> · D. K. Srivastava<sup>1</sup>

Received: 12 December 2018 / Accepted: 1 October 2019 / Published online: 29 October 2019  
© Springer Science+Business Media, LLC, part of Springer Nature 2019

## Abstract

This paper illustrates optimization and comparative analysis for rectangular microstrip patch antenna loaded with ‘T’-shape slot utilizing manual (conventional) optimization and particle swarm optimization (PSO) with curve fitting. Initially, a conventional antenna has been designed by cutting ‘T’-shape slot in rectangular radiating patch and manually optimized by selecting some parameters of patch as variable. The bandwidth and resonant frequency data obtained from IE3D simulation tool by varying distinct parameters of the conventional ‘T’-shape slot loaded antenna have been used for generating the curve in Graphmatica (curve fitting software) and developing the PSO program in MATLAB for optimization purpose. Finally, the PSO-optimized antenna has been attained and its performance has been compared with both initial conventional ‘T’-shape slot loaded antenna and manually optimized antenna. Fragmentary bandwidth of PSO-optimized ‘T’-shape slot loaded antenna has been increased by 16.86% as compared to initial conventional ‘T’-shape slot loaded antenna and kept the resonant frequency at 2.477 GHz near the desired frequency of 2.45 GHz.

**Keywords** Particle swarm optimization (PSO) · ‘T’-shape slot loaded · Curve fitting · Bandwidth · IE3D · MATLAB

## 1 Introduction

The advancement in wireless communication systems has raised the necessity for compact and low-profile antennas with wideband frequency band and high gain. Microstrip patch antenna has lot of benefits such as low profile, light weight and compactness; however, its fundamental disadvantages are their narrow bandwidth, low efficiency, lower gain and spurious feed radiation. There are lots of substrates that can be used to design microstrip antenna as [1] with a dielectric constant in the range 2.2–12. The lower dielectric constant substrate gives better efficiency along with large-scale bandwidth. Impedance bandwidth of patch antenna can be increased by employing various approaches just as taking different shapes and size of radiating patch, loading different types of slot and notches in the radiating patch.

The antenna size is highly essential for wireless conversation systems. The antenna bandwidth decreases as antenna size decreases, and this specialty limits the stuffed antenna design [2]. But, the operation of reduced size antenna must be equivalent to that of the normal antenna [3]. Many approaches have been suggested to achieve reduction in antenna size such as the utilization of dielectric substrates with high permittivity [4]. The antenna bandwidth can be raised by expanding the electrical path length of patch by optimizing its shapes [5]. Using of positioned notches on radiating patch and various patch shapes consisting slots and slits on patch result in antenna size reduction [6]. These changes increase the path of the surface current.

James Kennedy and Russell Eberhart interpreted the concept of particle swarm optimization in terms of its predecessor and reviewed the level of its growth from social simulation to optimize [7]. Islam et al. [8] have proposed an optimization of inverted E-shape design of microstrip patch antenna utilizing PSO with 15% bandwidth increment. Choukiker and Behera [9] have proposed an inset feed dual-band antenna design and optimization technique using particle swarm optimization with 33.54 MHz bandwidth. Rajpoot et al. [10] have enhanced the fractional bandwidth of microstrip antenna of I-shape patch by utilizing PSO

✉ Ramesh Kumar Verma  
ramesh85.ec@gmail.com

D. K. Srivastava  
dks1\_biet@rediffmail.com

<sup>1</sup> Department of Electronics and Communication Engineering,  
Bundelkhand Institute of Engineering and Technology,  
Jhansi, UP, India

optimization followed by curve fitting. Kibria et al. [11] have implemented modified particle swarm optimization (PSO) along with MATLAB and IE3D achieved 12% bandwidth rectification with 20.84% size reduction over a conventionally optimized antenna. Dey et al. [12] have presented an optimization technique used for resonant frequency between 3 and 18 GHz of gap-coupled rectangular microstrip antenna utilizing particle swarm optimization algorithm. Chang et al. [13] have designed an asymmetrical T-shape monopole dual-band simple antenna utilizing FR4 substrate for tuning the resonant frequency and bandwidth enhancement. Hu et al. [14] have presented a compact planner antenna loaded with a T-shape and two symmetrical edge resonators for multi-band (WLAN/WiMAX) applications. Keertana et al. [15] have designed a two T-shape symmetrical slot loaded multi-band microstrip antenna resonating at 4.84 GHz and 6.81 GHz frequency for UWB applications. Goel et al. [16] have designed an inverted T-shape antenna working in triple band for X-band applications. Ni et al. [17] have presented a multi-band T-shape antenna loaded with T-shape slots using line feed and coplanar waveguide (CPW) feed for WLAN and WiMAX applications. Murugan et al. [18] have designed an elliptical shape patch antenna loaded with T-shape slot utilizing FR4 substrate for multi-frequency operations. Reddy et al. [19] have designed a circularly polarized T-shape square patch antenna for WiMAX application resonating at 2.5 GHz and 9 GHz. Kumar et al. [20] have presented a band-notched T-shape slot loaded planar patch antenna with inset feed for UWB applications. Verma et al. [21] have designed a slotted T-shape patch antenna, and it has optimized by manual method for bandwidth enhancement.

The desire of wideband antenna design increases due to the increase in applications in wireless communication. Hence, it requires more and more bandwidth to cover the desire application, but microstrip antenna offers limited bandwidth. To overcome these limitations, slots and notches are cut in the patch. It is very important for designing of microstrip antenna to coincide with its resonant frequency precisely at design frequency due to its narrow bandwidth. Antenna can operate efficiently at resonant frequency in narrow band region. Thus, a methodology that matches the resonant frequency and boosts the bandwidth becomes more beneficial in antenna design.

In the current research methodology, the bandwidth of the proposed patch antenna design has been enhanced by optimization of different variable parameters of patch using PSO. PSO execution along with curve fitting and MATLAB has been analyzed to optimize the structure of patch antenna [22]. IE3D simulation tool [23] and Graphmatica software [24] have been utilized for antenna simulation and curve fitting while MATLAB has been utilized for optimization scheme. The proposed optimized antenna has been designed by glass epoxy (FR-4) substrate of dielectric constant 4.4 at frequency

2.45 GHz. Height and loss tangent ( $\tan\delta$ ) of the substrate material are 1.6 mm and 0.02, respectively. Initially, a conventional ‘T’-shape slot loaded antenna has been designed and then optimized by MATLAB using PSO program code.

## 2 Antenna geometry and design procedure

For antenna design, length and width of rectangular patch are evaluated by using Eqs. (1–4) [25]:

$$W = \frac{c}{2f_r} \sqrt{\frac{2}{\epsilon_r + 1}} \quad (1)$$

where  $f_r$  = design frequency in GHz,  $\epsilon_r$  is the dielectric constant of substrate,  $c = 3 \times 10^8$  m/s (speed of light) in vacuum and  $W$  is the width of patch.

Effective dielectric constant ( $\epsilon_{\text{reff}}$ ) of substrate material is evaluated by [25]:

$$\epsilon_{\text{reff}} = \frac{\epsilon_r + 1}{2} + \frac{\epsilon_r - 1}{2} \left(1 + \frac{12h}{W}\right)^{-\frac{1}{2}} \quad (2)$$

Extension length ( $\Delta L$ ) of the radiating patch is evaluated by [25]:

$$\frac{\Delta L}{h} = 0.412 \frac{(\epsilon_{\text{reff}} + 0.3) \left(\frac{W}{h} + 0.264\right)}{(\epsilon_{\text{reff}} - 0.258) \left(\frac{W}{h} + 0.8\right)} \quad (3)$$

Above value of extension length ( $\Delta L$ ) is used to evaluate the absolute length of the patch as given by [25]:

$$L = \frac{c}{2f_r \sqrt{\epsilon_{\text{reff}}}} - 2(\Delta L) \quad (4)$$

The calculated patch length ( $L_p$ ) and width ( $W_p$ ) are 28.83 mm and 37.26 mm, respectively. Ground length ( $L_g$ ) and width ( $W_g$ ) are evaluated by using Eqs. (5) and (6) as given by [25]:

$$L_g = 6h + L_p \quad (5)$$

$$W_g = 6h + W_p \quad (6)$$

The evaluated value of ( $L_g$ ) and ( $W_g$ ) is 38.43 mm and 46.86 mm, respectively.

The initial desired geometry of ‘T’-shape slot loaded patch antenna has been obtained by cutting slots  $L_1$ ,  $L_3$ ,  $W_1$  and  $W_3$  as shown in Fig. 1. The ground layer of the proposed antenna is beginning from bottom left edge of the radiating patch which has been considered as coordinate (0, 0). A microstrip line feed (50  $\Omega$ ) has been connected at bottom left edge of the radiating patch with a strip of length ( $L_2$ ) 3.5 mm and width ( $W_2$ ) 5 mm. The bandwidth and resonant frequency of initial ‘T’-shape slot loaded antenna could be

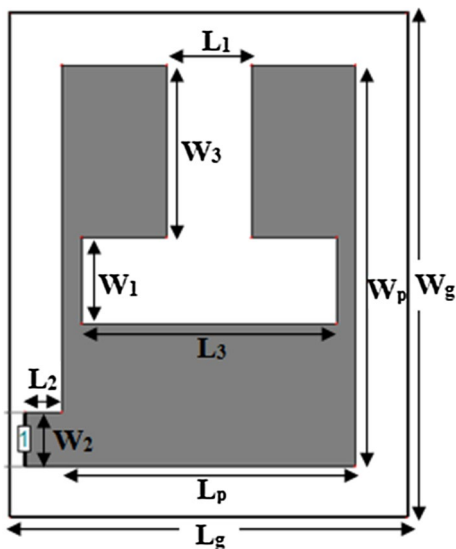


Fig. 1 Geometry of conventional ‘T’-shape slot loaded patch antenna

optimized by changing some parameters of antenna. All basic parameters [21] of initial ‘T’-shape slot loaded antenna are exhibited in Table 1.

The maximum bandwidth (less than  $-10$  dB) of conventional ‘T’-shape slot loaded patch antenna simulated by IE3D has been obtained 41.29% at 2.586 GHz resonant frequency with  $-22.09$  dB return loss when feed length and width are 3.5 mm and 5 mm, respectively. It has been simulated between 1 and 4 GHz for 1000 points. The lower and upper cutoff frequency of conventional antenna is 1.918 GHz and 2.916 GHz, respectively. Return loss graph of conventional ‘T’-shape slot loaded antenna is shown in Fig. 2. The fragmentary bandwidth (41.29%) and resonant frequency (2.586 GHz) of conventional ‘T’-shape slot loaded antenna are the intension of the optimization mechanism to amplify the above fragmentary bandwidth (FBW) through changing some parameters of the patch while preserving resonant frequency 2.586 GHz nearby desired frequency 2.45 GHz.

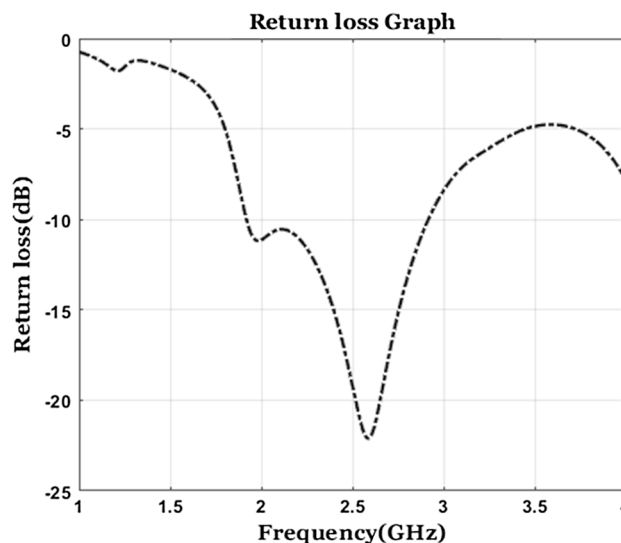


Fig. 2 Return loss graph of conventional ‘T’-shape slot loaded patch antenna

### 3 Optimization methods

Optimization of conventional ‘T’-shape slot loaded antenna has been performed by manual optimization (conventional optimization) as well as by particle swarm optimization (PSO) selecting some parameters of the antenna as variable. The selected variable parameters have been varied one by one keeping other constant in both optimization processes. Same variable parameters have been selected as variable for both optimization processes. The manual (conventional) optimization method has been performed by manually while PSO optimization method has been performed by curve fitting and MATLAB program. The performance of both manually optimized antenna and PSO-optimized antenna has been compared with conventional ‘T’-shape slot loaded antenna. For optimization of conventional ‘T’-shape slot loaded antenna, four parameters have been considered as variable for both optimizations.

Table 1 Basic parameters of ‘T’-shape slot loaded patch antenna

Substrate material (glass proxy)	$\epsilon_r = 4.4$ $h = 1.6$ mm
Rectangular ground plane (length and width)	$L_g = 38.43$ mm $W_g = 46.86$ mm
Rectangular patch (length and width)	$L_p = 28.83$ mm $W_p = 37.26$ mm
‘T’-shape slot parameter	$L_1 = 8$ mm, $L_3 = 24$ mm $W_1 = 8$ mm, $W_3 = 16$ mm
Feed line length	$L_2 = 3.5$ mm
Feed line width	$W_2 = 5$ mm
Feed position coordinate	(3.05, 7.3)

### 4 Manual (conventional) optimization

The conventional ‘T’-shape slot loaded antenna has been optimized by selecting four parameters  $L_1$ ,  $L_2$ ,  $W_1$  and  $W_2$  of the patch out of ten parameters  $L_g$ ,  $W_g$ ,  $L_p$ ,  $W_p$ ,  $L_1$ ,  $L_2$ ,  $L_3$ ,  $W_1$ ,  $W_2$  and  $W_3$  as listed in Table 1. Two parameters  $L_1$  and  $W_1$  are selected from ‘T’-shape slot (vertical and horizontal arm width), and remaining two parameters  $L_2$  and  $W_2$  are selected from feed strip line (feed strip length and width). The selected parameters have been varied separately one by one within their range without affecting others. The initial values, lower bound, upper bound and their step size

**Table 2** Range of variation in parameters

Selected parameters	Lower bound (mm)	Upper bound (mm)	Step size (mm)
$L_1$	4	14	1
$L_2$	1.7	4.1	0.2
$W_1$	2	14	1
$W_2$	3	9	0.5

**Table 3** Comparison between  $L_1, L_2, W_1$  and  $W_2$

Variable parameters	Resonant freq. (GHz)	Return loss (dB)	Bandwidth (%)
$L_1 = 12$ mm	2.628	-15.94	42.35
$L_2 = 2.5$ mm	2.402	-27.44	45.59
$W_1 = 4$ mm	2.646	-19.84	43.41
$W_2 = 7$ mm	2.640	-24.39	45.53

of variation in selected parameters are shown in Table 2. For each value of  $L_1, L_2, W_1$  and  $W_2$ , one antenna has been designed and simulated by IE3D. Lower cutoff frequency, upper cutoff frequency, resonant frequency and return loss have been noted for each value of parameters. Fragmentary bandwidth has been calculated for all antennas.

Initially,  $L_1$  varied from 4 to 14 mm in step of 1 mm. The initial value of  $L_1$  was 8 mm. Out of 11 different antennas (10 + 1 conventional), maximum bandwidth has been obtained 42.35% at resonant frequency 2.628 GHz with return loss -15.94 dB when  $L_1$  was 12 mm. Similarly, other variable parameters  $L_2, W_1$  and  $W_2$  are also varied in same manner.  $L_2$  is varied from 1.7 to 4.1 mm in step of 0.2 mm. Maximum bandwidth has been obtained 45.59% out of total 13 different antennas (12 + 1 conventional) at 2.402 GHz resonant frequency when  $L_2$  was 2.5 mm. Return loss of this antenna is -27.44 dB at its resonant frequency 2.402 GHz.  $W_1$  gives total 13 different antennas (12 + 1 conventional) when it is varied from 2 to 14 mm in step of 1 mm. Out of these antennas, one antenna has maximum bandwidth 43.41% when  $W_1$  was 4 mm. This antenna resonates at 2.646 GHz frequency with -19.84 dB return loss. Last variable parameter  $W_2$  is varied in step of 0.5 mm from 3 to 9 mm and gives total 13 different antennas (12 + 1 conventional). When  $W_2$  was 7 mm, antenna has maximum bandwidth 45.53% at 2.640 GHz resonant frequency with -24.39 dB return loss. These four selected antenna results out of 47(46 + 1 conventional) are exhibited in Table 3.

From Table 3, it can see that maximum bandwidth 45.59% has been obtained when parameter  $L_2$  was 2.5 mm. It means that when  $L_2$  was 2.5 mm, other three parameters were at its initial value. It also observed that resonant frequency 2.586 GHz

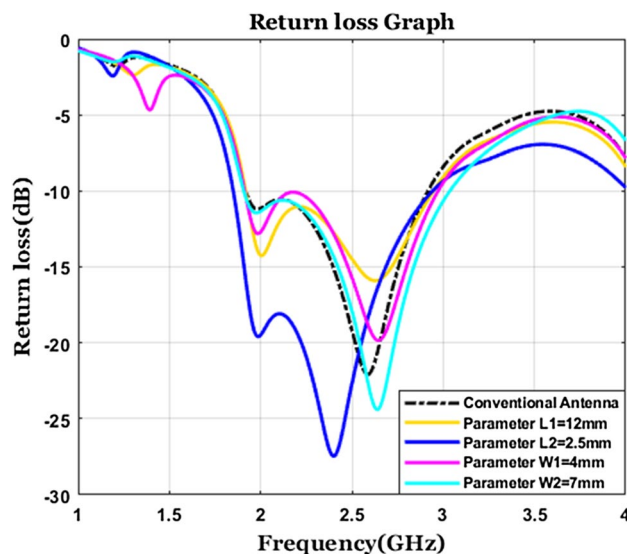


**Fig. 3** Comparative return loss versus frequency graph of different parameters

**Table 4** Comparison between conventional ‘T’-shape slot loaded antennas and manually optimized antenna

Parameters	Conventional ‘T’-shape slot loaded antenna	Manually (conventional) optimized antenna
Bandwidth (%)	41.29	45.59
Return loss (dB)	-22.09	-27.44
Fr (GHz)	2.586	2.402
VSWR	1.171	1.089

of conventional ‘T’-shape slot loaded antenna is shifted at 2.402 GHz which is close to design frequency 2.45 GHz. The comparative return loss graph is shown in Fig. 3. The manually optimized result has been compared with conventional ‘T’-shape slot loaded antenna result as exhibited in Table 4.

From Table 4, it can see that the bandwidth of antenna has enhanced. Return loss and VSWR of antenna also have improved. The resonant frequency also shifted toward desired frequency 2.45 GHz but not much close. Due to this, PSO optimization has been used to improve the results of conventional ‘T’-shape slot loaded antenna to large extent.

### 5 PSO algorithm

Particle swarm optimization (PSO) is a computational approach; population-based hypothetical optimization style is established in 1995 by Dr. Eberhart and Dr. Kennedy, encouraged by social nature of bird throng, fish schooling at the time of searching meal. An elementary PSO algorithm works by acquiring a population (called swarm) of candidate solutions

(called particles). These particles are reallocated over a search area in consonance with some simple and understandable formulae over the particle’s location and velocity. All particles displacement is affected by its neighborhood best known location and also supervised toward the most excellent known location in the search area that are upgraded at the time of better location found by alternative new particles. Displacement of particles is supervised through their individual best known location in the search area as well as the entire group best known location. PSO optimizes a problem by iteratively attempting to upgrade a candidate solution with reference to a given measure of quality. This is anticipated to move the swarm approaching toward the best solutions. The procedure is replicated, and doing so, it is expected; however, it not assured that an acceptable answer can eventually be recognized. Therefore, PSO begins with arbitrarily selected position and velocity of particles. Each and all particle attempts to reorganize its location utilizing the knowledge of the instant location, instant velocities, distance between instant location and personal best location ( $p_{best}$ ), also distance between instant location and global best location ( $g_{best}$ ) [7]. The key element for favorable outcome of PSO is particle’s velocity manipulation. Position adjustment of the particle will be mathematically formed [8, 9] according to the subsequence equation:

$$V_i(t + 1) = W * V_i(t) + C_1 * \delta_1 * (X_{p_{best}}(t) - X_i(t)) + C_2 * \delta_2 * (X_{g_{best}}(t) - X_i(t)) \tag{7}$$

where  $V_i(t)$  is the velocity of the particle in the  $i$ th dimension;  $X_i(t)$ , the particle’s coordinate in the  $i$ th dimension;  $t$ , the present iteration;  $W$ , the time-dependent weight constant that commonly reduces linearly from 0.9 to 0.6;  $C_1$  and  $C_2$ , the arbitrary constant, generally set at 2.0; and  $\delta_1$  and  $\delta_2$ , the arbitrary functions used independently to supply uniformly distributed counts between 0 and 1.

After the completion of iteration, present location of the particle is renovated [10] by next equation:

$$X_i(t + 1) = X_i(t) + V_i(t + 1) \tag{8}$$

The weighting function utilized in Eq. (7) is given as:

$$w = w_{Max} - \frac{(w_{Max} - w_{Min}) * Iter}{MaxIter} \tag{9}$$

where  $w_{Max}$  is the initial weight;  $w_{Min}$ , the final weight;  $MaxIter$ , the maximum iteration count; and  $Iter$ , the present iteration count

In an  $N$ -dimensional optimization issue, the calculations carry on for each dimension.  $X_{p_{best}}$  accounts  $i$ th particle’s location that obtains own personal best fitness value, whereas  $X_{g_{best}}$  accounts the position that obtains their global best fitness value among all.

## 6 Optimization applying PSO

The selected variable parameters (Table 2) of the antenna that specified for optimization such as length and width of feed strip and slot will form the position of the particle and initially choose a group of such kind of positions. Based on cost function, fitness value of each position has been evaluated. Cost function should be a function of position, and other antenna parameters should be set as input and desired characteristics of antenna. Based on the trait of the antenna, it can be single-objective oriented such as only bandwidth or resonant frequency or multi-objective oriented such as bandwidth and resonant frequency both. Four parameters  $L_1, L_2, W_1$  and  $W_2$  (selected for manual optimization) are held for PSO optimization purpose as listed in Table 2. The objective of the optimization mechanism is to amplify the fragmentary bandwidth (FBW) of conventional ‘T’-shape slot loaded antenna simulated above by changing these four parameters of the patch while preserving resonant frequency ( $f_r$ ) 2.586 GHz nearby desired frequency 2.45 GHz [8]. The variable parameters and range of variation are exhibited in Table 2.

## 7 Curve fitting

Graphmatica software (curve fitting) has been utilized to form the relationship between all varying parameter individually to BW and  $f_r$ . Each variable parameter has been varied uniformly one by one within their range while other three kept constant. For each value of  $L_1, L_2, W_1$  and  $W_2$ , one antenna has been designed and simulated by IE3D. Lower cutoff frequency, upper cutoff frequency, resonant frequency and return loss have been noted for each value of parameters. The selected variable parameters have been varied in same manner as in manual optimization, and fragmentary bandwidth has been calculated for all antennas.

Initially,  $L_1$  is varied from 4 to 14 mm in step of 1 mm. It creates 11 distinct antennas (10 + 1 conventional) to set up data for cost function. For same purpose,  $L_2$  is varied from 1.7 to 4.1 mm in step of 0.2 mm and gives total 13 (12 + 1 conventional) different antennas.  $W_1$  is varied from 2 to 14 mm in step of 1 mm and gives total 13(12 + 1 conventional) different antennas.  $W_2$  is also varied from 3 to 9 mm in step of 0.5 mm and gives total 13(12 + 1 conventional) different antennas.

The conventional ‘T’-shape slot loaded antenna is common among all variable parameter. Thus, a total 47(46 + 1 conventional) different antennas are available for evaluation. Fragmentary bandwidth (FBW) has been calculated for each antenna, and resonant frequency ( $f_r$ ) and return loss (RL) have been noted for all antenna. Some of them are shown in Table 5 as sample at their different values.

**Table 5** Variable parameter versus resonant frequency ( $f_r$ ) and FBW

Variation in parameter (value)	Resonant frequency (GHz)	Return loss (dB)	Fragmentary bandwidth (%)
$L_1$ (7 mm)	2.574	-24.59	40.17
$L_1$ (12 mm)	2.628	-15.94	42.35
$L_2$ (2.5 mm)	2.402	-27.44	45.59
$L_2$ (3.7 mm)	2.598	-19.78	29.12
$W_1$ (5 mm)	2.628	-20.65	42.78
$W_1$ (11 mm)	2.550	-22.09	40.30
$W_2$ (4.5 mm)	2.571	-21.20	40.33
$W_2$ (7 mm)	2.640	-24.39	45.53

A relationship between a particular variable parameter to FBW and  $f_r$  has been established by applying the values obtained from different antennas in Graphmatica (curve fitting software). Similarly, it has been followed for all other three parameters. The following set of Eqs. (10–17) are obtained that represent the relationship between  $L_1, L_2, W_1, W_2$  to FBW and  $f_r$ , FBW for  $L_1$

$$FBW_1 = 0.0008L_1^4 - 0.0242L_1^3 - 0.0409L_1^2 + 5.8848L_1 + 4.5264 \tag{10}$$

$f_r$  for  $L_1$

$$f_{r1} = -7.4912 \times 10^{-5}L_1^4 + 0.0005L_1^3 + 0.0082L_1^2 - 0.0597L_1 + 2.6113 \tag{11}$$

FBW for  $L_2$

$$FBW_2 = -0.1089L_2^4 - 0.6776L_2^3 + 1.0667L_2^2 + 16.7476L_2 + 11.6958 \tag{12}$$

$f_r$  for  $L_2$

$$f_{r2} = -0.0017L_2^4 - 0.0138L_2^3 + 0.0489L_2^2 + 0.9723 \tag{13}$$

FBW for  $W_1$

$$FBW_3 = 0.0025W_1^4 - 0.0249W_1^3 - 0.7209W_1^2 + 10.4964W_1 + 7.9603 \tag{14}$$

$f_r$  for  $W_1$

$$f_{r3} = -4.4951 \times 10^{-6}W_1^4 + 0.0001W_1^3 - 0.0003W_1^2 - 0.0203W_1 + 2.7301 \tag{15}$$

FBW for  $W_2$

$$FBW_4 = -0.0012W_2^4 - 0.0016W_2^3 + 0.0924W_2^2 + 1.8637W_2 + 30.6857 \tag{16}$$

$f_r$  for  $W_2$

$$f_{r4} = 2.3210 \times 10^{-5}W_2^4 - 0.0002W_2^3 - 0.0033W_2^2 + 0.0638W_2 + 2.3583 \tag{17}$$

### 7.1 Fitness function formation

Root mean square error-based fitness function has been utilized to generate the fitness function [8]. The following equation has been utilized to evaluate the root mean square error  $E_i$  of a particular program  $i$ :

$$E_i = \sqrt{1/n \sum_{j=1}^n (P_{ij} - T_j)^2} \tag{18}$$

where  $P_{ij}$  is the expected value by the particular program  $i$  for  $j$ th fitness case out of  $n$  fitness cases and  $T_j$  is the target value for  $j$ th fitness case. All  $P_{ij} = T_j$ , and thus,  $E_i = 0$  for a perfect fit. Utilizing the above RMSE-based fitness equation, our fitness function [10] was as follows:

$$F(x) = \sqrt{M(FBW - FBW_{target})^2 + N(f_r - f_{rtarget})^2} \tag{19}$$

where  $M$  and  $N$  are the biasing constant which controls the contribution of every term to the overall fitness function and  $FBW_{target}$  and  $f_{rtarget}$  are the desired bandwidth and desired resonant frequency. The generated PSO optimizes antenna toward the fragmentary bandwidth FBW by increasing the bias value  $M$  while PSO optimizes toward the resonating frequency  $f_r$  by increasing bias value of  $N$  [8].

### 8 Optimized results and discussion

Utilizing the relationship of Eqs. (10–17) and RMSE-based fitness function, a PSO program has been written and run it in MATLAB. The values of bias constant  $M$  and  $N$  have been set to 0.9 and 0.1 to giving more priority on bandwidth enhancement. We acquired the optimized values of variable parameters  $L_1, L_2, W_1$  and  $W_2$  after completing 200 iterations with 70 particles. The optimized values of  $L_1, L_2, W_1$  and  $W_2$  have been obtained 9.2347 mm, 2.5735 mm, 6.3210 mm and 5.2017 mm, respectively. The comparison between initial value and optimized value of parameters is exhibited in Table 6.

Conventional ‘T’-shape slot loaded antenna has been again designed at optimized value of the variable parameter

**Table 6** Comparison between initial value and PSO-optimized value of parameters

Parameter	Initial value	PSO-optimized value
$L_1$ (mm)	8	9.2374
$L_2$ (mm)	3.5	2.5735
$W_1$ (mm)	8	6.3210
$W_2$ (mm)	5	5.2017

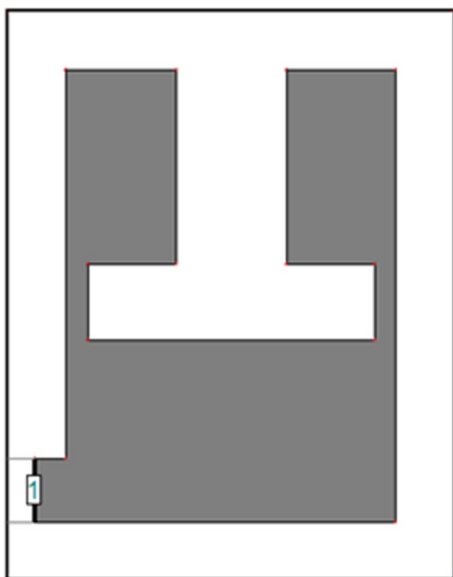


**Fig. 4** Geometry of PSO-optimized ‘T’-shape slot loaded patch antenna

**Table 7** Comparison between conventional ‘T’-shape slot loaded antenna and optimized antenna results

Parameter	Conventional ‘T’-shape slot loaded antenna	Manually (conventional) optimized antenna	PSO-optimized antenna
BW (%)	41.29	45.59	48.25
Fr (GHz)	2.586	2.402	2.477
RL (dB)	-22.09	-27.44	-44.32
VSWR	1.171	1.089	1.012

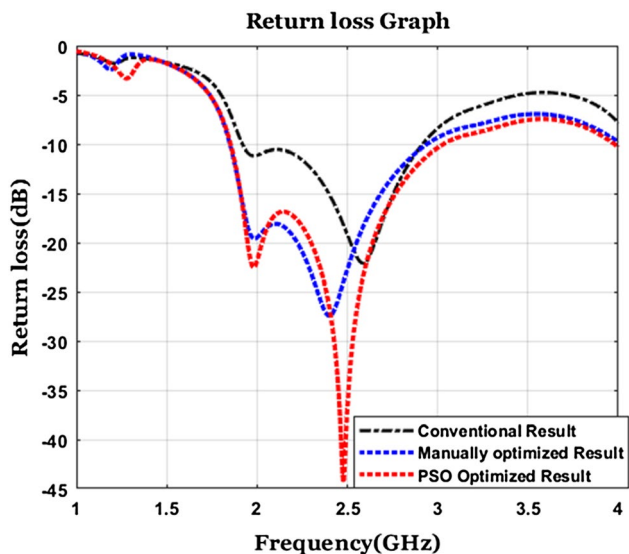


**Fig. 5** Comparative return loss graph of conventional ‘T’-shape slot loaded antenna and optimized antenna

and simulated through IE3D simulation tool. The geometry of the proposed PSO-optimized antenna design is shown in Fig. 4. The fragmentary bandwidth (FBW) of optimized antenna has been enhanced from 41.29 to 48.25%, and optimized antenna is resonating at 2.477 GHz near desire frequency 2.45 GHz with return loss -44.32 dB. The lower and upper cutoff frequency of PSO-optimized antenna is 1.854 GHz and 3.033 GHz, respectively. Bandwidth and return loss (RL) of optimized antenna have risen as compare to conventional ‘T’-shape slot loaded antenna. The PSO-optimized antenna result has been compared with

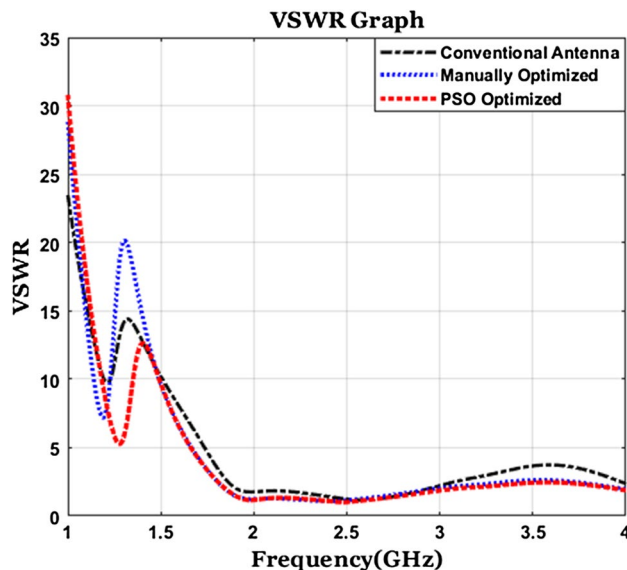


**Fig. 6** Comparative VSWR graph of conventional ‘T’-shape slot loaded and optimized antenna

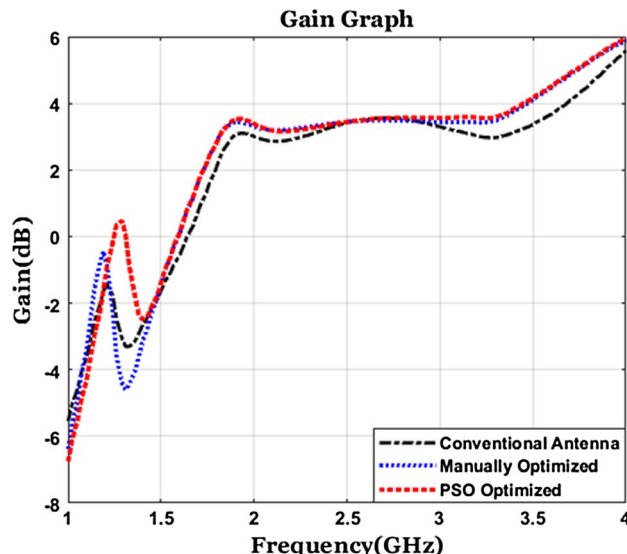


**Fig. 7** Comparative gain versus frequency graph of conventional ‘T’-shape slot loaded and optimized antenna

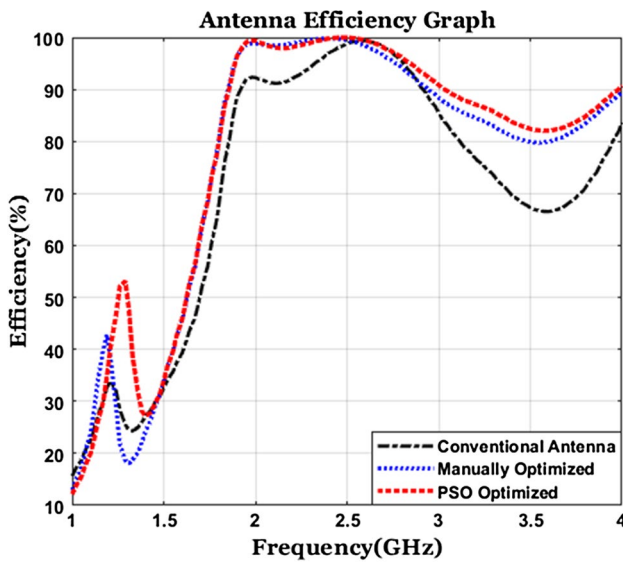


**Fig. 8** Comparative efficiency versus frequency graph of conventional ‘T’-shape slot loaded and optimized antenna

conventional ‘T’-shape slot loaded antenna and manually optimized antenna. The comparative result is exhibited in Table 7.

Return loss (dB), VSWR, gain (dB), efficiency (%), elevation plane ( $x-z$  plane) radiation pattern, azimuth plane ( $x-y$  plane) radiation pattern and field current distribution of the proposed optimized antenna have been analyzed at 2.477 GHz frequency. It is shown in Figs. 5, 6, 7, 8, 9, 10 and 11, and each graph is plotted for the frequency band from 1 to 4 GHz. Comparative return loss graph of conventional ‘T’-shape slot loaded antenna, manually optimized antenna and PSO-optimized antenna is shown in Fig. 5.

Figure 6 represents the comparative VSWR plot of conventional ‘T’-shape slot loaded antenna, manually

optimized antenna and PSO-optimized antenna. VSWR of conventional ‘T’-shape slot loaded antenna, manually optimized antenna and PSO-optimized antenna is lain in entire operating frequency range between 1 and 2. Smaller value of VSWR shows that the optimized antenna is more appropriately matched with transmission line and greater radiating power is delivered to the antenna. The value of VSWR of conventional ‘T’-shape slot loaded antenna and manually optimized antenna is 1.171 and 1.089 at resonant frequency 2.586 GHz and 2.402 GHz, respectively, while VSWR of PSO-optimized antenna is 1.012 at its resonant frequency 2.477 GHz which is remarkable. Figure 7 represents the antenna gain versus frequency plot of the conventional ‘T’-shape slot loaded antenna, manually optimized antenna and PSO-optimized antenna. Utmost antenna gain of conventional ‘T’-shape slot loaded antenna is 3.380 dB and 3.506 dB at frequency 2.477 GHz and 2.586 GHz, respectively. The gain of manually optimized antenna is 3.388 dB and 3.438 dB at 2.402 GHz and 2.477 GHz, respectively, while PSO-optimized antenna gain is 3.432 dB at resonant frequency 2.477 GHz. Antenna efficiency is defined as the ratio of radiated power ( $P_{rad}$ ) from the antenna to the power supplied ( $P_s$ ) to the antenna. It is frequency dependent and expressed in percentage. As represented in Fig. 8, the antenna efficiency of conventional ‘T’-shape slot loaded antenna is 98.44% and 99.38% at resonant frequency 2.477 GHz and 2.586 GHz, respectively. Antenna efficiency of manually optimized antenna is 99.81% and 99.61% at 2.402 GHz and 2.477 GHz, respectively, while PSO-optimized antenna has 99.99% antenna efficiency at resonant frequency 2.477 GHz. Figure 9a–c represents the elevation plane ( $x-z$  plane) radiation pattern of conventional ‘T’-shape slot loaded antenna, manually optimized antenna and PSO-optimized antenna at resonant frequency 2.586 GHz, 2.402 GHz and 2.477 GHz, respectively. 3 dB beam width

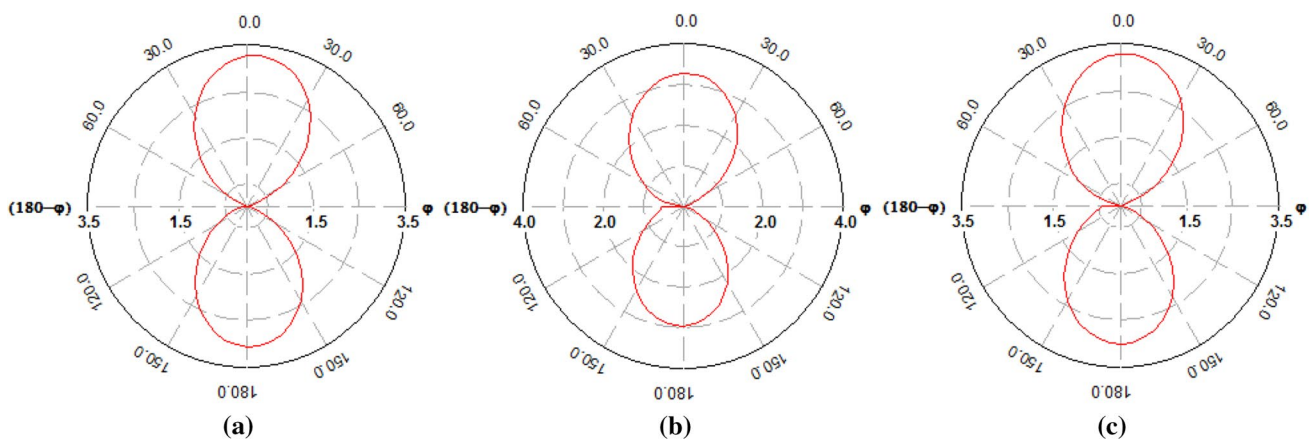


**Fig. 9** Elevation plane radiation pattern for **a** conventional ‘T’-shape slot loaded antenna at 2.586 GHz, **b** manually optimized antenna at 2.402 GHz, **c** PSO-optimized antenna at 2.477 GHz



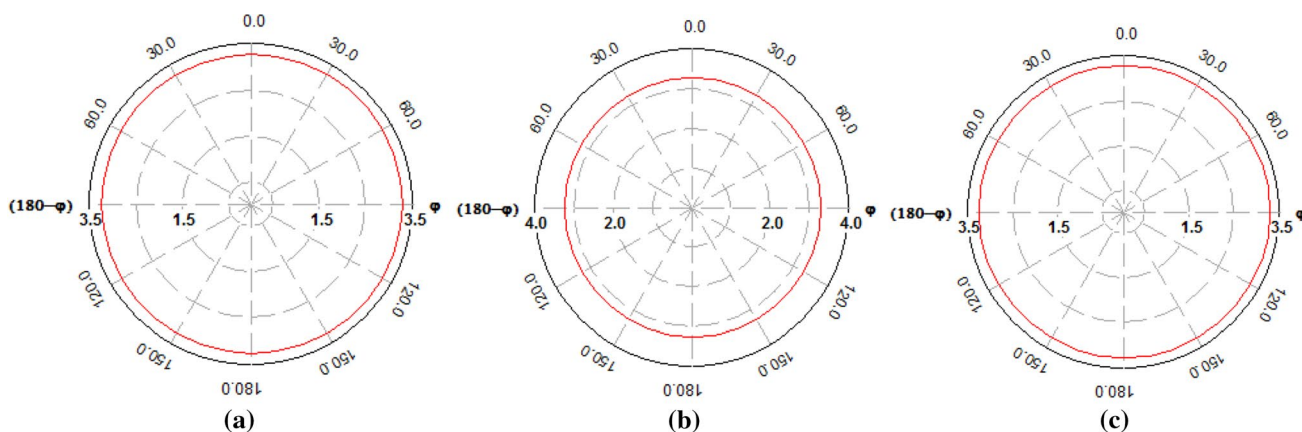


**Fig. 10** Azimuth plane radiation pattern for **a** conventional ‘T’-shape slot loaded antenna at 2.586 GHz, **b** manually optimized antenna at 2.402 GHz, **c** PSO-optimized antenna at 2.477 GHz

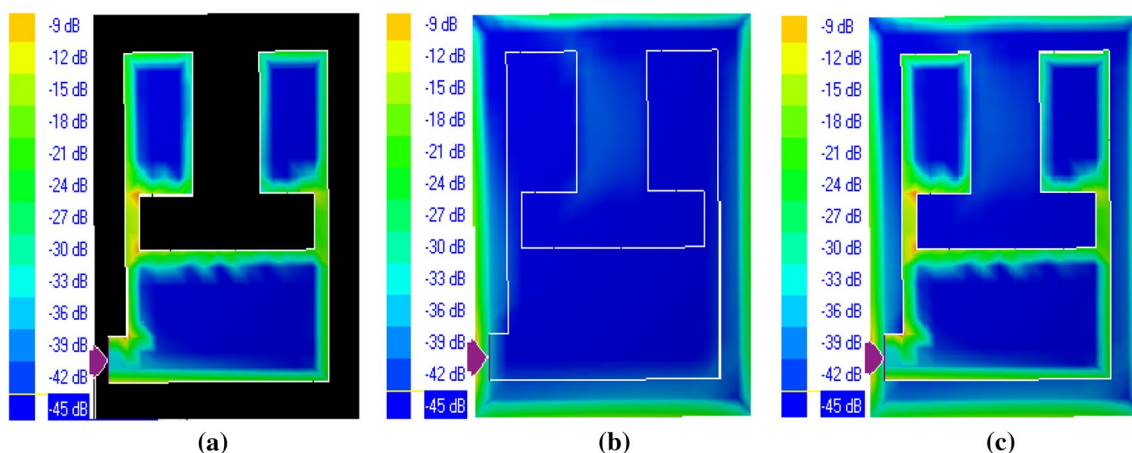


**Fig. 11** Field current distribution **a** electric field current distribution, **b** magnetic field current distribution, **c** electric and magnetic field current distribution, at 2.477 GHz

of the conventional ‘T’-shape slot loaded antenna and manually optimized antenna is  $82.032^\circ$  ( $55.536^\circ$ ,  $137.568^\circ$ ) and  $68.763^\circ$  ( $51.547^\circ$ ,  $120.310^\circ$ ) at resonant frequency 2.586 GHz and 2.402 GHz, respectively. PSO-optimized antenna has 3 dB beam width  $98.159^\circ$  ( $49.501^\circ$ ,  $147.660^\circ$ ) at resonant frequency 2.477 GHz. Figure 10a–c represents the azimuth plane ( $x$ – $y$  plane) radiation pattern of conventional ‘T’-shape slot loaded antenna, manually optimized antenna and PSO-optimized antenna at resonant frequency 2.586 GHz, 2.402 GHz and 2.477 GHz, respectively. In azimuth plane, radiation pattern is non-directional and circle passing through the maximum gain 3.253 dB, 3.275 dB and 3.279 dB at resonant frequency 2.586 GHz, 2.402 GHz and 2.477 GHz, respectively, for all angles. Energy radiated by the proposed PSO-optimized antenna in azimuth plane is equal in all direction. Figure 11a–c represents the field current distribution of PSO-optimized antenna at 2.477 GHz. Maximum E-current and M-current are 157.31(A/m) and 23,942(V/m) at resonant frequency 2.477 GHz.

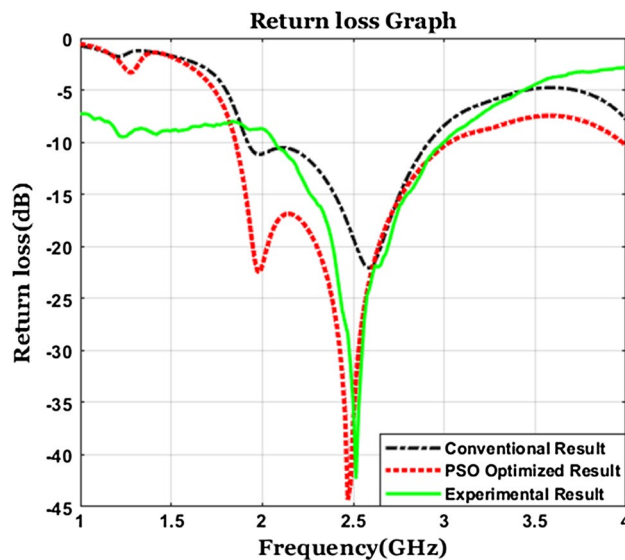
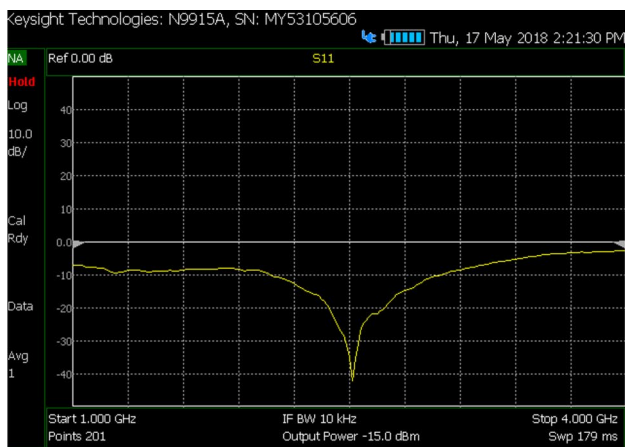


**Fig. 12** Comparative return loss plot of simulated and experimental result of antenna



(a)

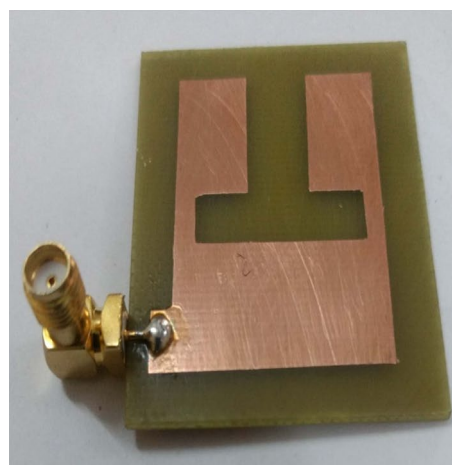


(b)

**Fig. 13** Experimental results **a** return loss versus frequency graph and **b** experimental setup for the proposed optimized antenna measured by spectrum analyzer

### 9 Experimental validation

For comparative analysis, simulated and experimental (measured) results of the proposed PSO-optimized antenna are shown in Fig. 12. The experimental impedance bandwidth of the proposed PSO-optimized antenna has been obtained 42.59% in the range of frequency 2.07–3.19 GHz at 2.53 GHz resonant frequency with return loss  $-39.198$  dB. The image of experimental return loss versus frequency plot and experimental setup for the proposed antenna measured



(a)



(b)

**Fig. 14** Prototype antenna design **a** patch view and **b** ground view

by spectrum analyzer are shown in Fig. 13a, b, respectively. Prototype antenna design patch view and ground view are shown in Fig. 14a, b, respectively.

### 10 Conclusion

The design, simulation, optimization, comparative analysis and reasonable execution of the proposed antenna have been introduced and scrutinized. The recommended microstrip antenna has been designed to overcome the inhibition of narrow bandwidth of the conventional patch antenna utilizing manual optimization and PSO. This paper talks about the optimization of fragmentary bandwidth of the proposed design of microstrip antenna attempt to expand

bandwidth and fix resonant frequency  $f_r$  near 2.45 GHz. In this work, PSO program has been created utilizing equations acquired by curve fitting. Utilizing the PSO program code, the fragmentary bandwidth of ‘T’-shape slot loaded patch antenna applicable in Bluetooth communication has been increased by 16.86%. The proposed PSO-optimized antenna has antenna efficiency 99.99% and 3.432 dB gain at resonant frequency 2.477 GHz. The value of VSWR of the optimized antenna is 1.012 at resonant frequency which

is much closer to ideal value 1.0. It is recognized that as a worldwide stochastic optimizer, PSO is especially reasonable for antenna optimizations which are typically quite nonlinear.

### Appendix

See Tables 8, 9, 10 and 11.

**Table 8** Variation in  $L_1=4-14$  mm (initial value = 8 mm)

Variable $L_1$ (mm)	Lower freq. (GHz)	Return loss (dB)	Resonant freq. (GHz)	Higher freq. (GHz)	Bandwidth (%)
4	2.161	-34.79	2.541	2.845	27.33
5	2.143	-41.74	2.553	2.867	28.90
6	2.117	-29.40	2.565	2.888	30.81
7	1.932	-24.95	2.574	2.903	40.17
8	1.918	-22.09	2.586	2.916	41.29
9	1.915	-20.03	2.595	2.927	41.80
10	1.913	-18.41	2.606	2.936	42.19
11	1.915	-17.02	2.616	2.941	42.26
12	1.917	-15.94	2.628	2.947	42.35
13	1.920	-15.10	2.012	2.948	42.24
14	1.925	-15.94	2.021	2.948	41.99

When  $L_1$  is varied from 4 to 14 mm in step of 1 mm, total 11 antennas (10+1 conventional) have been designed

**Table 9** Variation in  $L_2=1.7-4.1$  mm (initial value = 3.5 mm)

Variable $L_2$ (mm)	Lower freq. (GHz)	Return loss (dB)	Resonant freq. (GHz)	Higher freq. (GHz)	Bandwidth (%)
1.7	1.792	-23.99	1.934	2.637	38.16
1.9	1.807	-33.72	2.159	2.743	41.14
2.1	1.822	-34.60	1.982	2.844	43.81
2.3	1.836	-27.50	2.301	2.910	45.26
2.5	1.849	-27.44	2.402	2.941	45.59
2.7	1.864	-31.66	2.471	2.952	45.18
2.9	1.876	-54.20	2.520	2.949	44.48
3.1	1.889	-31.88	2.550	2.940	43.53
3.3	1.903	-25.54	2.574	2.929	42.47
3.5	1.918	-22.09	2.586	2.916	41.29
3.7	2.105	-19.78	2.598	2.903	29.12
3.9	2.234	-18.14	2.604	2.891	25.64
4.1	2.276	-16.91	2.610	2.880	23.43

When  $L_2$  is varied from 1.7 to 4.1 mm in step of 0.2 mm, total 13 antennas (12+1 conventional) have been designed

**Table 10** Variation in  $W_1 = 2\text{--}14$  mm (Initial value = 8 mm)

Variable $W_1$ (mm)	Lower freq. (GHz)	Return loss (dB)	Resonant freq. (GHz)	Higher freq. (GHz)	Bandwidth (%)
2	2.324	-17.52	2.697	3.008	25.66
3	2.249	-18.78	2.667	2.987	28.19
4	1.912	-19.84	2.646	2.972	43.41
5	1.915	-20.65	2.628	2.957	42.78
6	1.917	-21.31	2.613	2.943	42.22
7	1.917	-21.77	2.598	2.930	41.80
8	1.918	-22.09	2.586	2.916	41.29
9	1.917	-22.25	2.574	2.903	40.91
10	1.917	-22.27	2.562	2.889	40.45
11	1.914	-22.09	2.550	2.880	40.30
12	1.912	-21.87	2.538	2.858	39.66
13	1.912	-21.48	2.523	2.841	39.09
14	1.908	-20.94	2.511	2.822	38.65

When  $W_1$  is varied from 2 to 14 mm in step of 1 mm, total 13 antennas (12+1 conventional) have been designed

**Table 11** Variation in  $W_2 = 3\text{--}9$  mm (initial value = 5 mm)

Variable $W_2$	Lower freq. (GHz)	Return loss (dB)	Resonant freq. (GHz)	Higher freq. (GHz)	Bandwidth (%)
3	1.932	-18.65	2.520	2.809	36.99
3.5	1.930	-19.54	2.538	2.840	38.16
4	1.925	-20.39	2.552	2.866	39.24
4.5	1.920	-21.20	2.571	2.890	40.33
5	1.918	-22.09	2.586	2.916	41.29
5.5	1.915	-22.81	2.601	2.937	42.13
6	1.913	-23.49	2.613	2.956	42.84
6.5	1.909	-23.72	2.615	3.005	44.61
7	1.908	-24.39	2.640	3.036	45.63
7.5	1.905	-25.59	2.655	3.027	45.50
8	1.903	-26.20	2.664	3.020	45.38
8.5	1.901	-26.78	2.676	3.033	45.89
9	1.900	-27.44	3.685	3.045	46.31

When  $W_2$  is varied from 3 to 9 mm in step of 0.5 mm, total 13 antennas (12+1 conventional) have been designed

## References

- Balanis, C.A.: Antenna Theory, Analysis and Design. Wiley, New York (2005)
- Sun, C., Wu, Z., Bai, B.: A novel compact wideband patch antenna for GNSS application. *IEEE Trans. Antennas Propag.* **65**(12), 7334–7339 (2017)
- Kordzadeh, A., Kashani, F.H.: A new reduced size microstrip patch antenna with fractal shaped defects. *Progress Electromagn. Res. B* **11**, 29–37 (2009)
- Lo, T.K., Hwang, Y.: Microstrip antennas of very high permittivity for personal communications. In: Asia Pacific Microwave Conference, pp. 253–256 (1997)
- Wang, H.Y., Lancaster, M.J.: Aperture-coupled thin film superconducting meander antennas. *IEEE Trans. Antennas Propag.* **47**(5), 829–836 (1999)
- Waterhouse, R.: Printed Antennas for Wireless Communications. Wiley, New York (2007)
- Kennedy, J., Eberhart, R.: Particle swarm optimization. In: Proceedings of IEEE, International Conference on Neural Networks, vol. 4, pp. 1942–1948 (1995)
- Islam, M.T., Misran, N., Take, T.C., Moniruzzaman, M.: Optimization of microstrip patch antenna using particle swarm optimization with curve fitting. In: Proceedings of International Conference on Electrical Engineering and Informatics, Selangor, Malaysia, pp. 711–714 (2009)
- Choukiker, Y., Behera, S.K.: Design and optimization of dual band microstrip antenna using particle swarm optimization technique. *J. Infrared Millim. Terahertz Waves* **31**(11), 1346–1354 (2010)

10. Rajpoot, V., Srivastava, D.K., Saurabh, A.K.: Optimization of I-shape microstrip patch antenna using PSO and curve fitting. *J. Comput. Electron.* **13**(4), 1010–1013 (2014)
11. Kibria, S., Islam, M.T., Yatim, B., Azim, R.: A modified PSO technique using heterogeneous boundary conditions for broad band compact microstrip antenna designing. *Ann. Telecommun.* **69**, 509–514 (2014)
12. Dey, S., Sinha, A., Gill, B., Gangopadhyaya, M., Ray, S.: Resonant frequency optimization of rectangular gap coupled microstrip antenna using particle swarm optimization algorithm. In: *IEEE Conference*, pp. 1–4 (2016)
13. Chang, T.N., Jiang, J.H.: Meandered T-shaped monopole antenna. *IEEE Trans. Antennas Propag.* **57**(12), 3976–3978 (2009)
14. Hu, W., Yin, Y.Z., Yang, X., Fei, P.: Compact multiresonator-loaded planar antenna for multiband operation. *IEEE Trans. Antennas Propag.* **61**(5), 2838–2841 (2013)
15. Keertana, D.R., Murthy, M.V.S.D.N.N., Yeswanth, B., Rajasekhar, C., Kumar, D.N.: A novel multi frequency rectangular microstrip antenna with dual T shaped slots for UWB applications. *IOSR J. Electron. Commun. Eng.* **9**(1), 120–124 (2014)
16. Goel, A., Tripathy, M.R., Zaidi, S.A.: Design and simulation of inverted T-shaped antenna for X-band applications. *Int. J. Inf. Comput. Technol.* **4**(6), 565–570 (2014)
17. Ni, T., Jiao, Y.C., Weng, Z.B., Zhang, L.: T-shaped antenna loading T-shaped slots for multiple band operation. *Progress Electromagn. Res. C* **53**, 45–53 (2014)
18. Murugan, S., Rohini, B., Muthumari, P., Priya, M.P.: Multi-frequency T-slot loaded elliptical patch antenna for wireless applications. *ACES Express J.* **1**(7), 212–215 (2016)
19. Reddy, G.K., Kamadal, V.S., Punniamoorthy, D., Gopal, G.V., Poornachary, K.: T-shape microstrip patch antenna for WiMAX applications. In: *IEEE Conferences*, pp. 842–845 (2017)
20. Kumar, A., Singh, M.K.: Band-notched planar UWB microstrip antenna with T-shaped slot. *Radioelectron. Commun. Syst.* **61**(8), 371–376 (2018)
21. Verma, R.K., Srivastava, D.K.: Bandwidth enhancement of a slot loaded T-shape patch antenna. *J. Comput. Electron.* **18**(1), 205–210 (2019)
22. MATLAB and Simulink Version (2014)
23. Zeland Software Inc. “IE3D Electromagnetic Simulation and Optimization Package”
24. Graphmatica software by Keith Hertzner Copyright © 1992-2014 kSoft
25. Kumar, S., Gupta, H.: Design and study of compact and wide-band microstrip U-slot patch antenna for Wi-Max application. *IOSR J. Electron. Commun. Eng.* **5**(2), 45–48 (2013)

**Publisher’s Note** Springer Nature remains neutral with regard to jurisdictional claims in published maps and institutional affiliations.



**Ramesh Kumar Verma** is born on June 15, 1985, in Uttar Pradesh, India. He is currently pursuing PhD from AKTU, Lucknow, Uttar Pradesh, India. He had completed M.Tech. in the year 2015 from Bundelkhand Institute of Engineering and Technology, Jhansi, in Digital Communication. He had completed B.Tech. in the year 2009 from Raj Kumar Goel Institute of Technology, Ghaziabad, in Electronics and Communication Engineering.

He is an expert in antenna designing, fabrication, IE3D simulation software and particle swarm optimization (PSO) algorithm. Presently, he is working on optimization of microstrip patch antenna with PSO and curve fitting.



**Dr. D. K. Srivastava** is a Professor of Electronics and Communication Engineering in Bundelkhand Institute of Engineering and Technology (BIET), Jhansi. He has more than 15 years of experience in teaching, research and administrative work. He accomplished his PhD in Electronics Engineering in 2010; earlier, he obtained M.Tech. in Electronics Engineering in 1999 and B.Tech. in Electronics Engineering in 1994. Dr. Srivastava

has published more than 120 international/national research papers and supervised PhD and M.Tech. thesis. He is a reviewer in ‘Progress in Electromagnetic Research’ (PIER). He has long standing academic interests in microstrip antenna, digital electronics and optical communication. He had delivered many lectures/keynote address and chaired various technical sessions during nation and international conferences and training program.